J. Membrane Biol. 84, 117–126 (1985)

The Journal of
Membrane Biology

Monovalent Cation Permeabilities of the Potassium Systems in the Crab Giant Axon

M. Emilia Quinta-Ferreira, Bernat Soria and Eduardo Rojas
Department of Biophysics, School of Biological Sciences, University of East Anglia, Norwich, England, and Laboratory of Cell Biology and Genetics, NIADDK, NIH, Bethesda, Maryland 20205

Summary. Permeability ratios for pairs of monovalent cations permeating the two potassium systems proposed for the giant axon of the crab *Carcinus maenas* (M.E. Quinta-Ferreira, E. Rojas & N. Arispe, *J. Membrane Biol.* **66**:171–181, 1982*b*) were estimated from measurements of the reversal potential of the currents under voltage-clamp conditions. With K^+ inside the axon, permeability ratios from the reversal potential of the currents through the late channel are: $P_{Rb}/P_K = 0.9$, $P_{NH_4}/P_K < 0.2$ and $P_{Cs}/P_K = 0.18$. With Cs^+ inside the ratios are: $P_K/P_{Cs} = 8.7$, $P_{Rb}/P_{Cs} = 7.1$ and $P_{NH_4}/P_{Cs} = 2.4$. The analysis of the inward currents carried by Rb^+ or NH_4^+ showed similar reversal potentials for the early transient component and the late sustained component. Whence, the sequence of permeabilities for the two types of potassium channels is: $P_K > P_{Rb} > P_{NH_4} > P_{Na} = P_{Cs}$. The time constants for the activation of the two components recorded either in K-, Rb-, or NH_4-artificial seawater are twice as large as the corresponding time constants measured in Na-artificial seawater.

Key Words giant axon · potassium channel · crab axon · K-channel selectivity

Introduction

In a previous paper, the kinetic and steady-state characteristics of the outward currents measured under voltage-clamp conditions in crab nerve fibers were considered (Quinta-Ferreira et al., 1982*b*). The analysis of the outward current revealed two distinct components, a fast one, with activation-inactivation kinetics (here on referred to as the transient component) and a delayed one, with kinetics similar to those of potassium currents recorded in other nerve fibers (Hodgkin & Huxley, 1985*b*; Frankenhaeuser, 1962). This analysis of the outward currents in terms of two components lent support to the hypothesis that there are two different potassium channels in crab nerves. In this paper the selectivity of the two systems to several monovalent cations is compared. Rb^+, NH_4^+ and Cs^+ were chosen for study: NH_4^+ because ionic current measurements in squid giant axons showed that NH_4^+ is a current carrier for both the Na^+ and the K^+-conductance systems (Binstock & Lecar, 1969); Rb^+ because it is as good a current carrier as K^+ in the K-conductance in myelinated axons (Hille, 1973). These cations were found to be permeant in the two K^+ systems of the crab giant axon and relative permeabilities were calculated using the Goldman-Hodgkin-Katz equation (Goldman, 1943; Hodgkin & Katz, 1949) and measured reversal potentials.

Materials and Methods

A detailed description of the techniques used has been presented before (Quinta-Ferreira, Arispe & Rojas, 1982*a*).

Experimental Procedure

The giant axon was mounted in the experimental chamber as described in Quinta-Ferreira et al. (1982*a*). Of the four pools of the nerve chamber (Nonner, 1969), pool A was perfused with K-free-artificial seawater (K-free-ASW, *see* Table 1) while the axoplasm was equilibrated with either KF or CsF by diffusion from pools C and E (5 to 10 min).

A typical experimental protocol was as follows. First, a double-pulse series in K-free ASW to estimate the holding potential from the position of the Na-conductance inactivation curve. The holding potential was calculated assuming that, at a membrane potential of −70 mV, 30% of the Na-channels are inactivated. Next, the solution in pool A was replaced by a Na-free saline, with the test cation in place of Na^+. After five minutes a series of ionic currents was recorded under these conditions. The K-free ASW was re-introduced in pool A, and 10 to 15 min were allowed for recovery of the Na and/or K conductances. In the majority of the experiments the Na currents were partially restored.

Determination of Permeability Ratios

The permeability ratio for a given pair of monovalent cations was calculated using the Goldman-Hodgkin-Katz equation and mea-

Table 1. Composition of the solutions[a]

A. External chloride solutions	Na^+	K^+	Rb^+	X^+	Ca^{2+} (mM)	Mg^{2+}	$Tris^+$	Cl^-	TTX (nM)	Osmotic pressure (mOsm)
K-free ASW	470	—	—	—	12	14	10	532	150	935
K-ASW	—	480	—	—	12	14	10	542	300	965
X-ASW	—	—	—	470	12	14	10	532	300	912–976
B. Internal fluoride solutions	Cs^+	K^+	Na^+	$Tris^+$	Cl^- (mM)	F^-	EGTA	Dextran (%)		Osmotic pressure (mOsm)
KF	—	450	45	10	10	495	—	—		920
CsF-1	500	—	—	1	1	500	1	1		1200
CsF	450	—	45	10	10	495	—	—		960

[a] Osmotic pressure was measured using a vapor pressure osmometer (Wescor 5100C). The pH of external solutions ranged from 7.2 to 7.4 and the pH of the internal solutions ranged from 7.2 to 7.5. Activity coefficients for 500 mM solutions at 25°C as follows: NaCl, 0.681; KCl, 0.649; RbCl, 0.634; NH_4Cl, 0.649; KF, 0.67; NaF, 0.632; CsCl, 0.606 (from Robinson & Stokes, 1959).

sured values for the reversal potential, E_r. Reversal potential values were determined from experimental I-V_m curves as the potential at which the net flow of current is zero. Thus,

$$E_r = RT/F \ln \{[X]_o + (P_Y/P_X)[Y]_o\}/\{[X]_i + (P_Y/P_X)[Y]_i\} \quad (1)$$

where R, T and F have their usual meaning, P_Y represents the permeability of the cation Y and P_X the permeability of the reference cation X; $[X]_o$, $[X]_i$, $[Y]_o$ and $[Y]_i$ represent thermodynamic activities of the cations X and Y inside (i) and outside (o) the axon. The thermodynamic activities used were calculated from the activity coefficients (Robinson & Stokes, 1959).

Experimental Errors

With the voltage-clamp technique used in this work, the accuracy of the estimation of the permeability ratio is dependent on the accuracy of the determination of three parameters:
1) the absolute membrane potential,
2) the internal concentration of cations X and Y at the time when the reversal potential is measured, and
3) the leakage current at the reversal potential.

A way to avoid the requirement for parameters (1) and (2) is to determine the ionic selectivity ratio from the change in E_r upon change of the external solution in two consecutive runs. In this case one uses the following equation:

$$E_{r,Y} - E_{r,X} = RT/F \ln ((P_Y[Y]_o)/(P_X[X]_o)) \quad (2)$$

where the various parameters and symbols have the same meaning as for Eq. (1).

Correction of the current records for leakage currents is usually carried out assuming that the leakage current is not rectified. Whence, the current resulting from the addition of the responses to identical depolarizing (V_p) and hyperpolarizing (V_{-p}) pulses is assumed to represent specific ionic current. In the present series of experiments, for V_p smaller or equal to 50 mV, the current resulting from the addition of the responses to identical V_p and V_{-p} pulses was taken to represent specific ionic current. For V_p greater than 50 mV, the current record in response to a 50-mV hyperpolarizing pulse was scaled by a factor V_p/V_{-p} and subtracted from the record in response to V_p.

In some experiments with internal CsF a different leakage subtraction method was used. A current record in response to a small depolarizing pulse $V_{p,c}$ which did not elicit specific ionic currents, was scaled by a factor $V_p/V_{p,c}$ and subtracted from the current record in response to a larger depolarizing pulse V_p.

In the experiments with Cs^+ inside the axon accurate determination of the selectivity ratio from the reversal potential of the late component of the current was impossible. Due to internal accumulation of permeant cations caused by the inward currents, the concentrations $[X]_i$ and $[Y]_i$ could not be estimated.

Liquid Junction Potentials

There are two liquid junctions: between the agar bridge of the electrode C filled with 500 mM KCl plus 1 mM $CaCl_2$ (Ag-AgCl) and the solution in pool C; between the agar bridge of a similar electrode B and the solution in pool B. The net potential due to these two junctions was measured with electrodes in electrical contact with the solution in pools C and B and with an agar bridge (3 M KCl) electrically connecting the two pools (Baker, Hodgkin & Meves, 1964). These measurements showed that the net junction potentials were small (<2 mV). They were therefore ignored in the determination of the reversal potential.

Solutions

The ionic composition of the solutions used to measure the selectivity ratios is given in Table 1. To block the sodium conductance 150 or 300 nM TTX were added to the external solutions. TTX was kept at 4°C as a 230 μM stock solution. Test solutions in Table 1 are similar to the reference solution (K-ASW) with 470 mM cation X in place of 480 mM K^+. For simplicity they are called X-ASW, where X represents either Rb, NH_4, Cs or Na.

Rb-ASW was used as the control external solution in experiments designed to study the effects of external Na^+ on the potassium conductances. Thus the test solution was prepared by substituting the required quantity of Rb by Na.

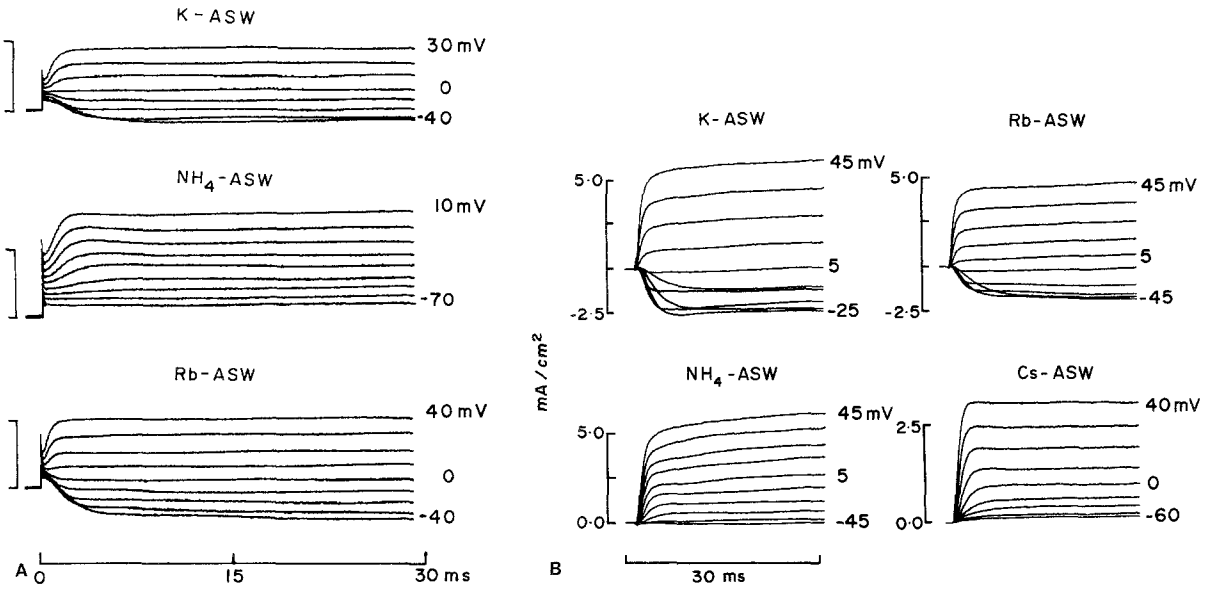

Fig. 1. Potassium, rubidium and ammonium currents through the early and delayed sustained potassium conductance systems. *A*. Total membrane currents in K-, NH_4- or Rb-ASW from experiment 810311A. Fiber cut in KF solution. Holding potential, −120 mV. The solution in pool A (at 14°C) is indicated above each set of current records. Absolute membrane potential during the depolarizing pulses is indicated next to three of the corresponding current records. Potential changed in 10-mV increments between the records. *B*. Specific membrane currents after subtraction of linear components. Current records in K-, Rb- or NH_4-ASW from experiment 810318A. Fiber cut in a KF solution. Holding potential, −95 mV. The solution in pool A (at 14°C) is indicated above each set of current records. Current records in Cs-ASW from experiment 810318B. Fiber cut in a KF solution. Holding potential, −100 mV. The numbers near some of the current records indicate the absolute membrane potential during the pulse. Voltage pulses were increased in 10-mV steps for the runs in K-, Rb- and NH_4-ASW. In Cs-ASW the first three records are associated with depolarizing pulses increasing in 20-mV steps

Results

Relative Permeabilities with Internal Potassium

Figure 1*A* depicts three sets of records of total membrane current in response to depolarizing voltage-clamp pulses. With K-ASW in pool A (upper part), the current record at 0 mV is almost flat, i.e. no inward or outward time varying components are apparent. This result suggests that 0 mV is the reversal potential for the K^+ currents through both, the early transient and the late sustained potassium conductances (i_{K1} and i_{K2} in Quinta-Ferreira et al., 1982*b*). It may also be seen in Fig. 1*A* that, with NH_4-ASW (middle part) the reversal potential is obtained near −60 mV. Again, the current record at −60 mV is flat, with no time-dependent components. In the presence of Rb-ASW the reversal potential for both potassium systems (i_{K1} and i_{K2}) is 5.4 mV.

Figure 1*B* shows four sets of records of specific ionic currents from two different experiments in which the internal solution was KF. Each membrane current record was corrected for linear components as explained in Materials and Methods. The solution in pool A is indicated above each set of records. With external K-ASW (top left) the current is inward for membrane potentials more negative than 5 mV. For more positive potentials the current is outward. With external Rb-ASW (top right) the situation is similar. This result indicates that Rb^+ passes through potassium channels about as easily as K^+.

In NH_4-ASW (bottom left), for the same range of membrane potentials, the inward currents are too small to measure and mainly outward currents are seen. In Cs-ASW (bottom right) the currents are always outward.

The reversal potential for the currents in K- and Rb-ASW can be determined from the corresponding current-voltage relationships. It was shown previously (Quinta-Ferreira et al., 1982*b*) that the currents can be analyzed in terms of two components and that at 18°C the first component is completely inactivated within 15 msec. Although the experiments presented in Fig. 1 were carried out at about 14°C, a temperature at which the time constants for the activation and inactivation processes are ex-

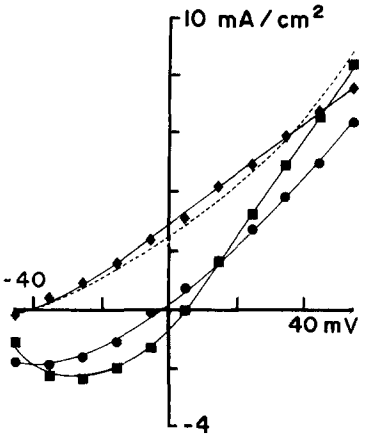

Fig. 2. Current-voltage curves at 30 msec with the axon in K-, Rb- and NH_4-ASW. Values of the current at 30 msec from same experiment as for Fig. 1*B*. Symbols as follows: ■, K-ASW; ●, Rb-ASW; ♦, NH_4-ASW. The solid lines were drawn through the points by eye. The dashed line was calculated from the currents recorded in K-ASW using Eq. (2) given in the text with $P_{NH_4}/P_K = 0.16$

Table 2. Relative permeabilities calculated from the reversal potential (internal Cs^+)

Experiment	Reversal potential E_r (mV)		
	K-ASW	Rb-ASW	NH_4-ASW
810311B	—	58.0	0.0
810313 (Figs. 6 & 7)	—	48.0	—
810318	—	32.0	—
810320 (Figs. 4 & 6)	51.0	50.0	39.0
810408 (Figs. 3 & 8)	50.0	45.0	10.0
810209 (Figs. 6 & 7)	58.0	—	—
Mean ± SD	54.7 ± 4.9	46.6 ± 9.5	24.5
	Permeability ratio P_Y/P_{Cs}		
810311B	—	10.6	1.0
810313A	—	7.1	—
810313B	—	3.7	—
810320	7.8	7.8	4.8
810408	7.4	6.6	1.5
810209	11.0	—	—
Mean ± SD	8.7 ± 2.0	7.1 ± 2.5	2.4

pected to be larger, the last 5 msec of 30-msec records were considered to represent K^+ current flowing through the delayed system. Whence, the values of the current for the I-V_m curves were measured at 30 msec, unless otherwise noted. It is assumed that at this time only the delayed channels are conducting and, therefore, the reversal potentials measured are used to determine the selectivity of that system of K-channels exhibiting delayed activation. The membrane current records shown in Figs. 1*A* and 1*B* can be used to check whether or not the reversal potential for the other component of the potassium currents (the early transient component) is similar to that of the late sustained component.

Figure 2 shows the I-V_m curves calculated from the membrane current records shown in Fig. 1*B*. It can be seen that the reversal potential in Rb-ASW is 6 mV smaller than the reversal potential in K-ASW and that in NH_4-ASW is approximately −40 mV. With a value for the difference $E_{r,Y}$-$E_{r,X}$ obtained from Fig. 2, solving Eq. (2) for P_Y/P_X, one gets $P_{Rb}/P_K = 0.8$ and $P_{NH_4}/P_K = 0.16$. It should be noted that in the experiments with external NH_4^+ and internal K^+ the inward currents were very small and, therefore, the reversal potential $E_{r,Y}$ could not be determined accurately.

The analysis of the currents recorded in NH_4-ASW may be further complicated by side effects of the external NH_4-ASW. It has been shown that an increase in internal pH occurs due to entry of NH_3 (Boron & De Weer, 1976; Mullins et al., 1983). Although the solution in pools C and E was buffered with 10 mM Tris Cl, it is possible that the pH of the axoplasm in pool A increased, causing an increase in the leakage conductance (Rojas & Atwater, 1968).

Two experiments in which K-ASW and Rb-ASW were tested in the same axon gave different $E_{r,Rb}$ values, namely 7 mV (experiment 810311A) and −4.4 mV (experiment 810318). As the reversal potential measured in K-ASW was greater than the reversal potential calculated assuming that the activity coefficient for potassium inside the axon is identical to that in the solutions in pools C and E, the potential E_r measured in Rb-ASW was adjusted by adding 1.6-$E_{r,K}$ to $E_{r,Rb}$. Since the permeability sequence calculated from these two $E_{r,Rb}$ values (−4.4 and 7 mV) is opposite in each experiment, it is impossible to draw a quantitative conclusion about the ratio P_{Rb}/P_K.

Relative Permeabilities with Internal Caesium

The results indicate that although NH_4^+ is a current carrier for the delayed K systems, this cation is significantly less permeant than Rb^+. In order to increase the size of the inward NH_4^+ currents, experiments were performed using CsF as the internal solution (*see* Table 1).

Figure 3 shows three sets of records of ionic currents from one experiment in which the external solution was either K-ASW (upper part), NH_4-ASW (middle part) or Rb-ASW (lower part). In this ex-

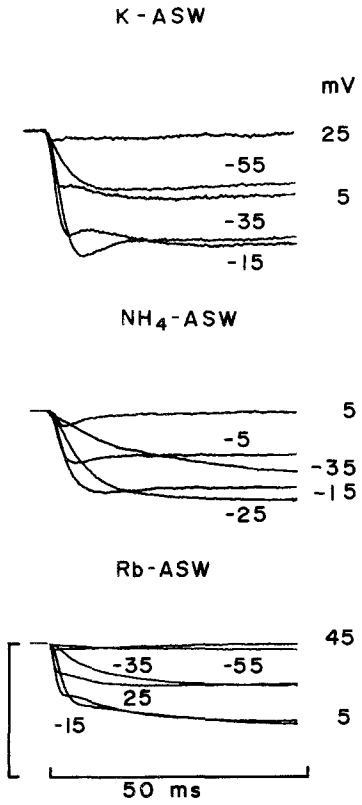

Fig. 3. Potassium, rubidium and ammonium inward currents. Experiment 810408: cut ends of the fiber in a CsF solution. Holding potential, −95 mV. The solution in pool A (at 14°C) is indicated above each set of current records. Vertical calibration: 2.5 mA/cm² for runs in K- and Rb-ASW; 1.3 mA/cm² for runs in NH_4-ASW.

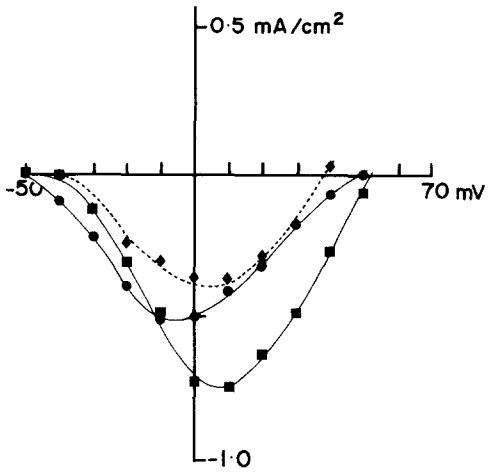

Fig. 4. Current-voltage curves at 30 msec with the axon in K-, Rb- or NH_4-ASW. Experiment 810320: cut ends of the fiber in CsF solution and holding potential −90 mV. Solution in pool A at 14°C as follows: ■, K-ASW; ●, Rb-ASW; ♦, NH_4-ASW. The dashed curve was calculated with Eq. (3) from the values of the currents in K-ASW and using P_K/P_{Cs} = 7.8 and P_{NH_4}/P_{Cs} = 4.8

periment 10 consecutive runs were made, five in Rb-ASW, one in K-ASW, two in Rb-ASW and two in NH_4-ASW. To obtain each current trace shown on Fig. 3, four inward current records were averaged (1 sec between the sweeps). It may be seen that inward currents are present in the three cases. It should also be noticed that with Cs^+ inside the size of the inward currents is larger than in the experiments with K^+ inside (compare the set of records in the middle part of Fig. 3 with the set shown in the lower part, left side, in Fig. 1*B*). It is possible that some Rb^+, K^+ and NH_4^+ accumulated inside the segment of the fiber in pool A. For this reason any outward component of the currents (*not shown*) should not be attributed to Cs^+ alone and the reversal potentials determined should be considered as lower limits.

For the experiment illustrated in Fig. 3 relative permeabilities calculated using Eq. (1) (and reversal potentials from the corresponding I-V_m curves) are: P_K/P_{Cs} = 7.4, P_{Rb}/P_{Cs} = 6.6 and P_{NH_4}/P_{Cs} = 1.5. From these ratios one can calculate P_{Rb}/P_K = 0.89 and P_{NH_4}/P_K = 0.2. These derived ratios are larger than those calculated directly with the data in Fig. 2 and Eq. (2), namely 0.8 and 0.16, respectively.

Figure 4 illustrates the I-V_m curves for an axon with the cut ends in CsF solution and bathed in K-ASW (■), Rb-ASW (●) or NH_4-ASW (◇). It may be seen that in NH_4-ASW the current reverses at a potential approximately 10 mV smaller than in K-ASW. The relative permeability P_{NH_4}/P_{Cs} is calculated as 4.8 while P_K/P_{Cs} equals 7.8.

For the currents in Rb-ASW, the reversal potential is 50 mV and the permeability ratio P_{Rb}/P_{Cs} is 7.7. Here again, the derived ratios, namely, P_{Rb}/P_K = 0.99 and P_{NH_4}/P_K = 0.62, are greater than the ratios calculated directly from the data in Fig. 2.

Table 2 summarizes the data available. It may be seen that Rb^+ is as good a current carrier as K^+ in the delayed system and that NH_4^+ can pass through the delayed system more easily than Cs^+. Since in all the experiments the current record at the reversal potential of the delayed system did not exhibit time-dependent components, i.e. no inward or outward components of the specific ionic currents could be detected, it seems logical to consider that this potential was also the reversal potential for the early transient component.

In order to determine if currents in NH_4-ASW (I') can be predicted from the currents in K-ASW (I) using the independence principle (Hodgkin & Huxley, 1952*a*), the following equation, similar to that in Binstock and Lecar (1969), was used:

$$\frac{I'}{I} = \frac{\{\alpha[X]'_o + \beta[Y]'_o - (\beta[Y]'_i + [Z]'_i)\exp(FV/RT)\}}{\{\alpha[X]_o + \beta[Y]_o - (\beta[Y]_i + [Z]_i)\exp(FV/RT)\}} \quad (3)$$

Table 3. Kinetic and steady-state parameters for the inward current components[a]

(a) V_M (mV)	(b) τ_{n_1} (msec)	(c) τ_{h_K}	(d) $-i_{K_1,peak}$	(e) $-i_{K_1,max}$ (mA/cm²)	(f) τ_{n_2} (msec)	(g) $-i_{K_2,max}$ (mA/cm²)	V_H (mV)	Temp (°C)
1) Internal K^+								
810315 (K-ASW)								
−50	4.1	4.0	1.27	13.00	5.5	1.73	−120	14.0
−40	3.3	5.7	3.80	18.75	7.4	3.91		
−20	2.2	4.6	3.11	13.86	5.1	4.03		
810314 (Rb-ASW)								
−60	4.9	29.3	0.83	1.46	17.3	0.46	−120	14.5
−50	3.2	23.4	0.80	1.15	14.2	0.64		
−40	2.3	11.2	0.78	1.73	9.0	0.91		
−30	1.8	6.8	0.64	1.65	6.4	0.88		
2) Internal Cs^+								
810209 (K-ASW)								
0	3.1	3.4	1.58	12.80	4.4	3.84	−130	13.0
10	2.5	3.9	1.60	9.28	4.1	3.52		
20	2.3	3.8	1.54	8.80	4.0	3.36		
30	2.7	3.7	1.38	8.96	4.0	2.88		
40	2.3	2.5	0.89	7.20	3.2	2.56		
810320 (NH_4-ASW)								
−30	4.7	5.9	0.14	0.80	7.1	0.19	−90	14.0
−10	4.6	5.7	0.31	2.01	6.3	0.43		
0	3.3	3.5	0.33	2.77	5.3	0.53		
+10	2.3	2.8	0.38	—	4.6	0.55		
810313 (Rb-ASW)								
−57	4.7	24.0	0.09	0.18	14.7	0.11	−117	14.0
−47	4.8	11.9	0.15	0.48	10.6	0.25		
−37	4.0	6.1	0.20	1.13	7.8	0.37		
−17	1.9	5.0	0.23	0.57	6.6	0.59		

[a] In experiments performed at temperatures different from 14°C time constants were corrected for this temperature assuming a Q_{10} of 3. (e): i_{K_1} values corrected for inactivation. (g): maximum i_{K_2} values.

where $[\ ]_o$ represents chemical activity outside, $[\ ]_i$ chemical activity inside the fiber, Z represents the reference cation, $\alpha = P_X/P_Z$, $\beta = P_Y/P_Z$ and F/RT has the same meaning as for Eq. (1).

The values obtained are plotted against membrane potential in Fig. 4 (dashed curve). It can be seen that the agreement between the predicted and the experimental values is good, indicating that under the experimental conditions used here the independence principle is obeyed.

For the currents in Rb-ASW, although the reversal potential is similar to that in K-ASW (*see* Fig. 4), the measured currents are smaller than the values calculated using Eq. (3).

Separation of Inward Potassium, Rubidium and Ammonium Currents into Two Components

Inward currents in K-, Rb- or NH_4-ASW exhibited complex kinetics which could be analyzed in terms of an early transient plus a delayed component.

Shown in Fig. 5 is the analysis of two records made in K-ASW (left side) and of three records made in Rb-ASW (right side). In both cases the internal solution was KF. It may be seen that after an initial peak value, the current decreases and then settles to a higher steady value. The last 10 msec of the inward current records shown in Fig. 5 (used to calculate the steady-state value and to generate the delayed component) are likely to contain a small but significant contribution from the transient component. For this reason the separation of the two components of the currents is not as accurate as in the case of outward currents recorded with K-free ASW in pool A. The solid lines represent fitted curves which provide a reasonable description of the experimental points.

With internal Cs^+ instead of K^+, larger inward currents were recorded in NH_4-ASW. The analysis of some of these current records, together with the records of inward currents recorded in K- or Rb-ASW are presented in Fig. 6. Again, the measured currents (represented by the points) are well described by the sum of two components (the solid

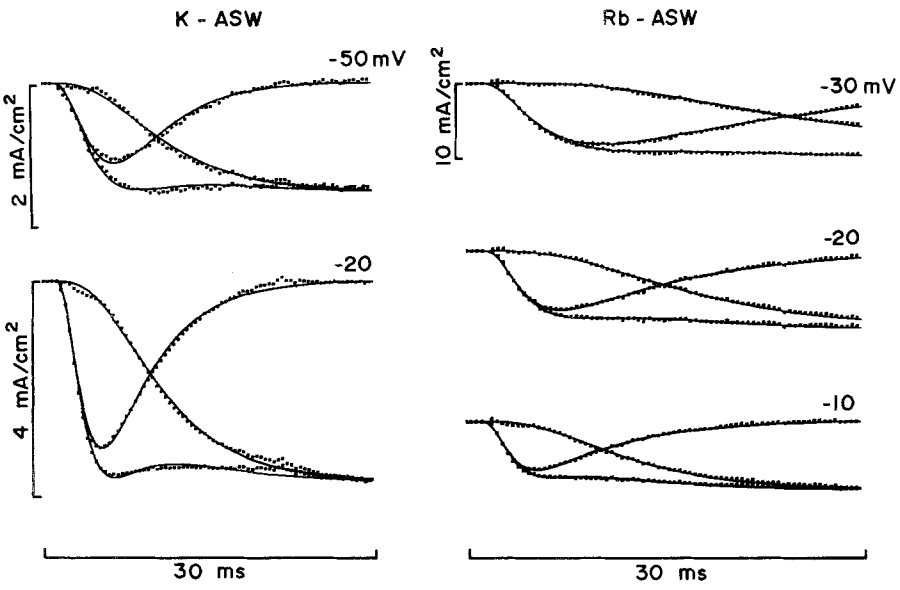

Fig. 5. Analysis of the inward currents recorded with the fiber in K- or Rb-ASW. *Left side:* Experiment 810315 with KF inside the axon. Solution in pool A, K-ASW at 14°C. *Right side:* Experiment 810314 with KF inside the axon. Solution in pool A, Rb-ASW at 14.5°C. Absolute membrane potential during the pulses is given in mV next to each set of records. Interval between points = 100 μsec. Solid lines represent fitted curves obtained as described in Quinta-Ferreira et al. (1982*b*)

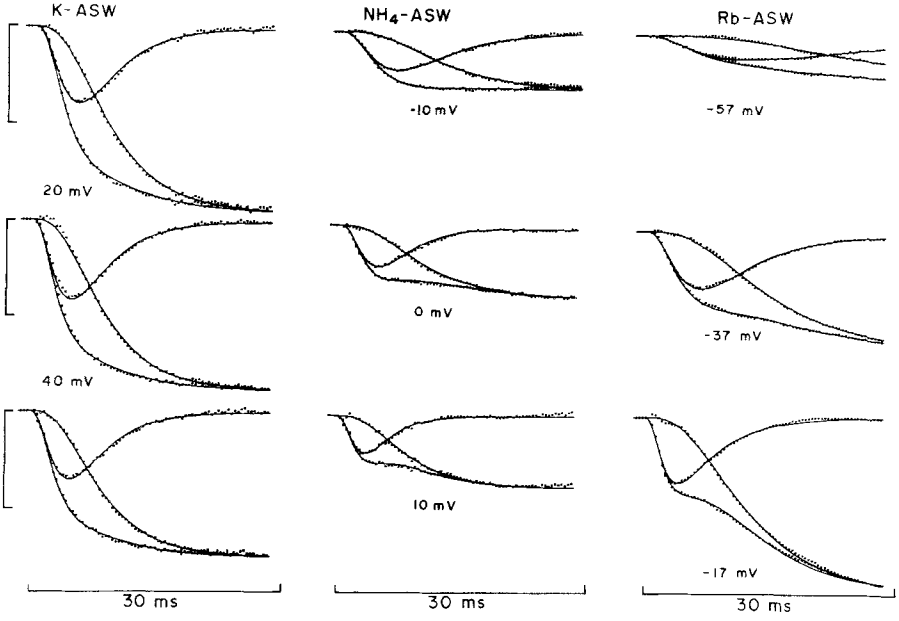

Fig. 6. Analysis of the inward currents carried by potassium, rubidium or ammonium. *Left side:* currents recorded with the fiber in K-ASW at 13°C. Experiment 810209. Holding potential −130 mV. Vertical calibration: 2 mA/cm². *Middle:* currents recorded with the fiber in NH_4-ASW at 14°C. Experiment 810320. Holding potential −90 mV. Vertical calibration: 0.45 mA/cm². *Right side:* currents recorded with the fiber in Rb-ASW at 14°C. Experiment 810313. Holding potential −117 mV. Vertical calibration: 0.35 mA/cm². For the three fibers the internal solution was CsF. Solid lines represent fitted curves

lines represent fitted curves). Based on these results, it can be concluded that Rb^+ and NH_4^+ are permeant in both potassium systems.

The activation time constants of the currents obtained from the separation of the two components (as illustrated in Fig. 6) are plotted as a function of membrane potential in Fig. 7.

In this figure, the points corresponding to membrane potentials more negative than −18 mV were obtained from the analysis of inward currents in Rb-ASW (●). Those in the range from −30 to 10 mV were obtained from the analysis of records made in NH_4-ASW (◆) and the points at positive membrane potentials represent data in K-ASW (■). The dashed line was calculated using the empirical rate constant functions described in Quinta-Ferreira et al. (1982*b*). The values were adjusted to 14°C assuming a Q_{10} of 3 and the calculated time constants were multiplied by 2. Numerical values are given in Table 3.

In general the activation time constants decrease gradually as the membrane potential is made more positive in much the same way as the time constants for the outward currents (Quinta-Ferreira et al., 1982*b*). This observation suggests that the rate at which channels open in the presence of high

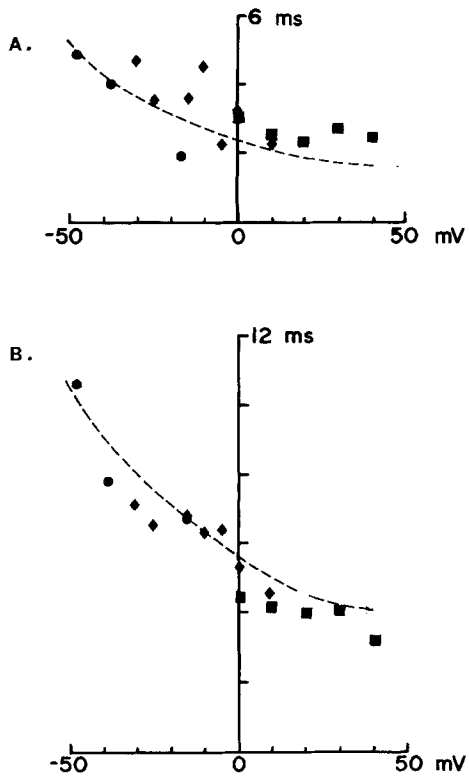

Fig. 7. Voltage dependence of the activation time constants. *A*. Activation time constant for transient component of the currents. ●, Experiment 810313 from Fig. 6; ♦, Experiments 810320 (from Fig. 6) and 810408; ■, Experiment 810209 from Fig. 6. All time constants were adjusted to 14°C assuming a Q_{10} of 3. Dashed line was calculated using the empirical equations for the rate constants given in Quinta-Ferreira et al. (1982*b*) divided by 2. *B*. Activation time constants for the delayed component. Values from the same experiments as in part *A*. Dashed line: calculated using the empirical equation given in Quinta-Ferreira et al. (1982*b*). This curve was corrected to take into account the temperature difference (factor 1.55) and multiplied by 1.95

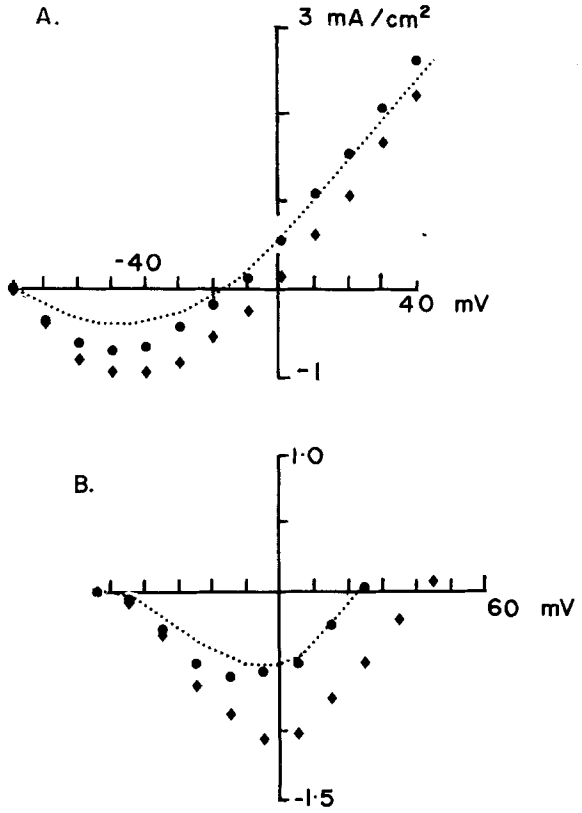

Fig. 8. Effects of external sodium on the delayed inward and outward currents. *A*. Experiment 810314: holding potential −120 mV. Cut ends of the fiber in a KF solution, ♦, Rb-ASW at 14.5°C; ●, 235 mM Rb + 235 mM Na-ASW. The dotted curve was obtained from the values of the currents in Rb-ASW using Eq. (3) in the text with $P_{Rb}/P_K = 1$ and $P_{Na}/P_K = 0.0$. *B*. Experiment 810408: holding potential −95 mV. Internal CsF. Temperature 14°C. The dotted curve was obtained from the values of the currents at 60 msec in Rb-ASW using Eq. (3) and $P_{Rb}/P_{Cs} = 6.0$ and $P_{Na}/P_{Cs} = 0.0$. ♦, Rb-ASW; ●, 235 mM Rb + 235 mM Na-ASW

concentrations of either K^+, Rb^+ or NH_4^+ is half of that measured in K-free ASW.

Effects of External Sodium Ions

The experiments presented in the preceding section were designed to measure permeability ratios. They were performed using an ASW in which all the Na^+ was replaced by a given test cation. To measure any possible blocking effects of the cation *X* not predicted by Eq. (3), experiments were carried out in which the concentration of Na^+ was varied keeping the sum $[Na^+]_o + [X^+]_o$ constant at 470 mM.

Shown in Fig. 8 are four I-V_m curves obtained with either internal K^+ (*A*) or Cs^+ (*B*). The dotted curves were calculated using Eq. (3). For positive membrane potentials there is excellent agreement between the measured and predicted values. At negative membrane potentials, however, the measured currents are greater than the predicted values. The most likely explanation for this discrepancy is that at 30 msec, when the currents were measured, the transient component was still present.

It may be tentatively concluded, therefore, that the external application of Na^+ does not block the cation flow in the delayed system. In the case of internal application of Na^+, however, the situation is quite different (*see* Quinta-Ferreira et al., 1982*b*). The reduction in outward potassium currents with internal application of 150 mM Na^+ is greater than that predicted on the basis of the independence principle. The I-V curve measured with 150 mM Na^+ plus 350 mM K^+ inside exhibits saturation as the membrane potential reaches 50 mV during the pulse. This phenomenon has also been observed in

the squid giant axon (Bezanilla & Armstrong, 1972). This asymmetrical response of the membrane to the application of Na^+ suggests that there are internal sites in both types of potassium channels with greater affinity for Na^+ than for K^+.

Discussion

The most important conclusion from the work reported in this paper is that Rb^+, NH_4^+ and Cs^+ are permeant in the two K^+-conductance systems of the crab giant axon (Connor, Walter & McKown, 1977; Quinta-Ferreira et al., 1982*b*). Both systems showed similar relative permeabilities calculated using the Goldman-Hodgkin-Katz equation and measured reversal potentials.

Permeability Sequence in Crab Axon Compared with that in Other Preparation

Both in the squid giant axon at rest (Hagiwara et al., 1972) and in the delayed K^+ channel of the node of Ranvier (Hille, 1973) and of the squid giant axon (Chandler & Meves, 1965; Moore et al., 1966; Binstock & Lecar, 1969), the sequence of permeabilities appears to be: $P_K > P_{Rb} > P_{NH_4} > P_{Cs} = P_{Na}$. The sequence found in this study is identical.

While the ratio P_{NH_4}/P_K in this work was found to be smaller than 0.2, for the squid giant axon larger values are reported, namely 0.26 (Binstock & Lecar, 1969) and 1.0 (Moore et al., 1966).

The average P_{Cs}/P_K value obtained from Table 2 is 0.11. This selectivity ratio is larger than the values reported for other preparations (Gorman, Woolum & Cornwall, 1982). However, it should not be forgotten that this value was obtained from the reversal potential in experiments with CsF inside. The concentration of the permeant K^+ inside was taken as zero. During the inward K^+ currents, a substantial increase in K^+ concentration inside the axon took place which, when taken into account in the calculations with Eq. (1), should decrease this value.

Effects of External Potassium, Rubidium and Ammonium on Kinetic Parameters

We have seen that the rate constants for activation of the potassium systems are halved in K-ASW (*see* Fig. 7). Similar results have been obtained in the squid giant axon (Swenson & Armstrong, 1981) who showed that K^+ channels close more slowly in either high K^+- or Rb^+-ASW. One possible explanation for this effect is that external K^+ interacts with the gating structure of the channels. The dependence of channel gating on the nature and concentration of the external permeant cations has been reported in various preparations. In squid giant axons an increase in external potassium not only reduces the rate of K^+ channel closing (Swenson & Armstrong, 1981) but also reduces the rate of inactivation of the sodium conductance, and its steady-state value (Adelman & Palti, 1969). In myelinated nerve fibers high external K^+ reduces the rate at which the potassium conductance is turned off on repolarization (Dubois, 1981). On the other hand, the kinetic parameters of chemically activated channels are also affected by certain external cations (Marchais & Marty, 1979).

Swenson and Armstrong (1981) proposed that the K^+ channels are prevented from closing when K^+ (or Rb^+) ions occupy a site close to the external entrance to the channel.

Assuming a two-state transition for the activation gates (Tsien & Noble, 1969), it has been shown that the forward and backward rate constants are given by the equations

$$\alpha(V) = \exp[(a(1 - \chi)(V - V_o) - \delta\varepsilon)kT] \quad (4a)$$

$$\beta(V) = \exp[(-a\chi(V - V_o) - \delta\varepsilon)kT] \quad (4b)$$

where a represents the effective valence of the gates, χ is a reaction coordinate such that $0 < \chi < 1$, V_o represents the transition potential and $\delta\chi$ represents the nonelectrostatic contribution to the energy barrier (Rojas, 1975). A reduction in the value of the rate constants may be induced by either a reduction in the effective valence a or by an increase in the size of the nonelectrostatic contribution to the energy barrier $\delta\varepsilon$. Figure 7 clearly shows that, in the range from -50 to $+50$ mV the voltage dependence of $(\alpha + \beta)^{-1}$ determined in K-ASW is similar to that determined in Na-ASW. It is likely, therefore, that the parameter affected is $\delta\varepsilon$, as any change in the effective valence a, the transition potential V_o or the fraction of the electric field acting on the gates would change the slope of the dashed curve in Fig. 7 and its position on the voltage axis.

This research was supported by the Science Research Council of the U.K. The authors are pleased to thank Dr. C. Collins for reading the manuscript and for valuable comments.

References

Adelman, W.J., Palti, Y. 1969. The influence of external potassium on the inactivation of sodium currents in the giant axon of the squid *Loligo pealei*. *J. Gen. Physiol.* **53**:685–703

Baker, P.F., Hodgkin, A.L., Meves, H. 1964. The effect of diluting the internal solution on the electrical properties of a perfused giant axon. *J. Physiol. (London)* **170**:541–560

Bezanilla, F., Armstrong, C.M., 1972. Negative conductance caused by entry of sodium and caesium ions into the potassium channels of squid giant axons. *J. Gen. Physiol.* **60**:588–608

Binstock, L., Lecar, H. 1969. Ammonium ion conductance in the squid giant axon. *J. Gen. Physiol.* **53**:342–361

Boron, W.F., De Weer, P. 1976. Intracellular pH transients in squid axons caused by CO_2, NH_3 and metabolic inhibitors. *J. Gen. Physiol.* **67**:91–112

Chandler, W.K., Meves, H. 1965. Voltage clamp experiments on internally perfused giant axons. *J. Physiol. (London)* **180**:788–820

Connor, J.A., Walter, D., McKown, R. 1977. Neural repetitive firing. Modifications of the Hodgkin-Huxley axon suggested by experimental results from crustacean axons. *Biophys. J.* **18**:81–102

Dubois, J.M. 1981. Evidence for the existence of three types of potassium channels in the frog Ranvier node membrane. *J. Physiol. (London)* **318**:297–316

Frankenhaeuser, B. 1962. Instantaneous potassium currents in myelinated nerve fibers of *Xenopus laevis*. *J. Physiol. (London)* **160**:46–53

Goldman, D.E. 1943. Potential, impedance and rectification in membranes. *J. Gen. Physiol.* **27**:37–60

Gorman, A.L.F., Woolum, J.C., Cornwall, C.M. 1982. Selectivity of the Ca-activated and light-dependent K channels for monovalent cations. *Biophys. J.* **38**:319–322

Hagiwara, S., Eaton, D.G., Stuart, A.E., Rosenthal, N.P. 1972. Cation selectivity of the resting membrane of squid axon. *J. Membrane Biol.* **9**:373–384

Hille, B. 1973. Potassium channels in myelinated nerve: Selective permeability to small cations. *J. Gen. Physiol.* **61**:669–686

Hodgkin, A.L., Huxley, A.F. 1952*a*. The dual effect of membrane potential on sodium conductance in the giant axon of *Loligo*. *J. Physiol. (London)* **116**:497–506

Hodgkin, A.L., Huxley, A.F. 1952*b*. A quantitative description of membrane current and its application to conduction and excitation in nerve. *J. Physiol. (London)* **117**:500–544

Hodgkin, A.L., Katz, B. 1949. The effect of sodium ions on the electrical activity of the giant axon of the squid. *J. Physiol. (London)* **108**:37–77

Marchais, D., Marty, A. 1979. Interaction of permeant ions with channels activated by acetylcholine in *Aplysia* neurones. *J. Physiol. (London)* **297**:9–45

Moore, J.W., Anderson, N.G., Blaustein, M.P., Takata, M., Lettvin, J.Y., Pickard, W.F., Bernstein, T., Pooler, J. 1966. Alkali cation specificity of squid axon membrane. *Ann. N.Y. Acad. Sci.* **137**:818–829

Mullins, L.J., Tiffert, G., Vassort, G., Whittembury, J. 1983. Effects of internal sodium and hydrogen ions and of external calcium ions and membrane potential on calcium entry in squid axons. *J. Gen. Physiol.* **338**:295–319

Nonner, W. 1968. A new voltage clamp method for Ranvier nodes. *Pfluegers Arch.* **309**:176–192

Quinta-Ferreira, M.E., Arispe, N., Rojas, E. 1982*a*. Sodium currents in the giant axon of the crab *Carcinus maenas*. *J. Membrane Biol.* **66**:159–169

Quinta-Ferreira, M.E., Rojas, E., Arispe, N. 1982*b*. Potassium currents in the giant axon of the crab *Carcinus maenas*. *J. Membrane Biol.* **66**:171–181

Robinson, R.A., Stokes, R.H. 1959. Electrolyte Solutions. Butterworths, London (second edition)

Rojas, E. 1975. Gating mechanism for the activation of sodium conductance in nerve membranes. *Cold Spring Harbor Symp. Quant. Biol.* **XL**:305–320

Rojas, E., Atwater, I. 1968. An experimental approach to determine membrane charges in squid giant axons. *J. Gen. Physiol.* **51**:131s–145s

Swenson, R.P., Armstrong, C.M. 1981. K channels close more slowly in the presence of external K and Rb. *Nature (London)* **291**:427–429

Tsien, R.W., Noble, D. 1969. A transition state theory approach to the kinetics of conductance changes in excitable membranes. *J. Membrane Biol.* **1**:248–273

Received 30 April 1984; revised 29 October 1984